Peak grain forecasts for the US High Plains amid withering waters

Assaad Mrad[a,1], Gabriel G. Katul[a], Delphis F. Levia[b,c], Andrew J. Guswa[d], Elizabeth W. Boyer[e,2], Michael Bruen[f,2], Darryl E. Carlyle-Moses[g,2], Rachel Coyte[a,2], Irena F. Creed[h,2], Nick van de Giesen[i,2], Domenico Grasso[j,2], David M. Hannah[k,2], Janice E. Hudson[b,2], Vincent Humphrey[l,2], Shin'ichi Iida[m,2], Robert B. Jackson[n,o,p,2], Tomo'omi Kumagai[q,2], Pilar Llorens[r,2], Beate Michalzik[s,2], Kazuki Nanko[m,2], Catherine A. Peters[t,2], John S. Selker[u,2], Doerthe Tetzlaff[v,w,2], Maciej Zalewski[x,y,2], and Bridget R. Scanlon[z]

[a]Nicholas School of the Environment, Duke University, Durham, NC 27708; [b]Department of Geography & Spatial Sciences, University of Delaware, Newark, DE 19716; [c]Department of Plant and Soil Sciences, University of Delaware, Newark, DE 19716; [d]Picker Engineering Program, Smith College, Northampton, MA 01063; [e]Department of Ecosystem Science and Management, Pennsylvania State University, University Park, PA 16803; [f]School of Civil Engineering, University College Dublin, Dublin 4, Ireland; [g]Department of Geography and Environmental Studies, Thompson Rivers University, Kamloops, BC V2C 0C8, Canada; [h]School of Environment and Sustainability, University of Saskatchewan, Saskatoon, SK S7N 5C8, Canada; [i]Faculty of Civil Engineering and Geosciences, Delft University of Technology, 2628 CN Delft, Holland; [j]Office of the Chancellor, University of Michigan-Dearborn, Dearborn, MI 48128; [k]School of Geography, Earth and Environmental Science, University of Birmingham, Birmingham B15 2TT, United Kingdom; [l]Division of Geological and Planetary Sciences, California Institute of Technology, Pasadena, CA 91125; [m]Department of Disaster Prevention, Meteorology and Hydrology, Forestry and Forest Products Research Institute, Tsukuba 305-8687, Japan; [n]Department of Earth System Science, Stanford University, Stanford, CA 94305; [o]Woods Institute for the Environment, Stanford University, Stanford, CA 94305; [p]Precourt Institute for Energy, Stanford University, Stanford, CA 94305; [q]Graduate School of Agricultural and Life Sciences, University of Tokyo, Tokyo 113-8657, Japan; [r]Institute of Environmental Assessment and Water Research, Consejo Superior de Investigaciones Científicas, 08034 Barcelona, Spain; [s]Institute of Geography, Friedrich Schiller University of Jena, 07743 Jena, Germany; [t]Department of Civil and Environmental Engineering, Princeton University, Princeton, NJ 08544; [u]Department of Biological & Ecological Engineering, Oregon State University, Corvallis, OR 97331; [v]Leibniz Institute of Freshwater Ecology and Inland Fisheries, 12587 Berlin, Germany; [w]Department of Geography, Humboldt University of Berlin, 1248 Berlin, Germany; [x]European Regional Center for Ecohydrology, United Nations Educational, Scientific and Cultural Organization, 90-364 Lodz, Poland; [y]Department of Applied Ecology, University of Lodz, 90-136 Lodz, Poland; and [z]Bureau of Economic Geology, Jackson School of Geosciences, The University of Texas at Austin, Austin, TX 78758

Edited by Peter H. Gleick, Pacific Institute for Studies in Development, Environment, and Security, Oakland, CA, and approved August 31, 2020 (received for review April 30, 2020)

Irrigated agriculture contributes 40% of total global food production. In the US High Plains, which produces more than 50 million tons per year of grain, as much as 90% of irrigation originates from groundwater resources, including the Ogallala aquifer. In parts of the High Plains, groundwater resources are being depleted so rapidly that they are considered nonrenewable, compromising food security. When groundwater becomes scarce, groundwater withdrawals peak, causing a subsequent peak in crop production. Previous descriptions of finite natural resource depletion have utilized the Hubbert curve. By coupling the dynamics of groundwater pumping, recharge, and crop production, Hubbert-like curves emerge, responding to the linked variations in groundwater pumping and grain production. On a state level, this approach predicted when groundwater withdrawal and grain production peaked and the lag between them. The lags increased with the adoption of efficient irrigation practices and higher recharge rates. Results indicate that, in Texas, withdrawals peaked in 1966, followed by a peak in grain production 9 y later. After better irrigation technologies were adopted, the lag increased to 15 y from 1997 to 2012. In Kansas, where these technologies were employed concurrently with the rise of irrigated grain production, this lag was predicted to be 24 y starting in 1994. In Nebraska, grain production is projected to continue rising through 2050 because of high recharge rates. While Texas and Nebraska had equal irrigated output in 1975, by 2050, it is projected that Nebraska will have almost 10 times the groundwater-based production of Texas.

crop production | groundwater | Hubbert curve | Ogallala aquifer | peak water

Today, more than half of the world population lives in countries where aquifers are overpumped primarily for crop irrigation (1, 2). This casts doubt on the ability to continue to produce enough crops to sustain the burgeoning global population and the increasing water intensities of their changing diets (3, 4). Reliable projections of future harvests and groundwater availability must ideally anticipate simultaneous water and food shortages and provide a framework for assessing intervention and mitigation options.

The High Plains Aquifer (HPA), which includes the Ogallala aquifer, underlies eight states in the central United States and supplies more than 3 billion US dollars worth of groundwater-based production (2007 estimate; ref. 5). The northern HPA has seen no significant decline in groundwater levels (6), yet many

Significance

Rapid groundwater depletion represents a significant threat to food and water security because groundwater supplies more than 20% of global water use, especially for crop irrigation. A large swath of the US High Plains, which produces more than 50 million tons of grain yearly, depends on the Ogallala aquifer for more than 90% of its irrigation needs. A predator–prey-type model serves as a minimalist representation of groundwater use–crop production dynamics. It explains and predicts reductions in groundwater withdrawal on three High Plains states and subsequent declines in irrigated crop production. The model shows how recharge rates and the adoption of irrigation technologies control these trends. It also provides a general framework for assessing groundwater-based irrigation sustainability.

Author contributions: A.M., G.G.K., D.F.L., and B.R.S. designed research; A.M., A.J.G., and M.B. performed research; A.M., G.G.K., D.F.L., A.J.G., N.v.d.G., V.H., C.A.P., and B.R.S. analyzed data; and A.M., G.G.K., D.F.L., A.J.G., E.W.B., M.B., D.E.C.-M., R.C., I.F.C., N.v.d.G., D.G., D.M.H., J.E.H., V.H., S.I., R.B.J., T.K., P.L., B.M., K.N., C.A.P., J.S.S., D.T., M.Z., and B.R.S. wrote the paper.

The authors declare no competing interest.

This article is a PNAS Direct Submission.

[1]To whom correspondence may be addressed. Email: mradassaad2@gmail.com.

[2]E.W.B., M.B., D.E.C.-M., R.C., I.F.C., N.v.d.G., D.G., D.M.H., J.E.H., V.H., S.I., R.B.J., T.K., P.L., B.M., K.N., C.A.P., J.S.S., D.T., and M.Z. contributed equally to this work.

This article contains supporting information online at https://www.pnas.org/lookup/suppl/doi:10.1073/pnas.2008383117/-/DCSupplemental.

First published October 5, 2020.

areas overlying the central and southern HPA are experiencing groundwater withdrawal rates far exceeding their recharge rates (6, 7). Given the large imbalance between withdrawals and recharge, groundwater resources in the central and southern HPA may be reasonably approximated as nonrenewable. Thus, the HPA provides an experimental paragon for the differing levels of interaction between groundwater withdrawals, groundwater recharge, and crop production, the largest groundwater user in the HPA (8).

Previous projections of the future of groundwater withdrawals in the HPA were inspired by Hubbert's (9) 1962 analysis of US crude oil production. Hubbert foreshadowed the peak in oil production that occurred in the mid-1970s (10), and, now, the symmetric curve describing the rise, peak, and fall in oil production is known as the "Hubbert curve." The idea of fitting nonrenewable resource use trends with a "Hubbert curve" has since gained prominence (11, 12), and an analogy between oil production and groundwater withdrawals was used to suggest the inevitability of peak nonrenewable water withdrawal (hereafter, peak water) as a parallel to peak oil (13). Hubbert-like groundwater withdrawal patterns have been documented in many regions around the world (e.g., numerous basins in India, the North China Plains, California's Central Valley) where groundwater withdrawals are much higher than their recharge (13). Moreover, forecasts of HPA groundwater extraction and future availability have benefited from fitting measurements of well water levels with the logistic function, the antiderivative of the Hubbert curve (14, 15).

While the analogy between the Hubbert curve and groundwater depletion has received empirical support and some acceptance, a mechanistic explanation of why groundwater withdrawal trends should follow the Hubbert curve, a curve symmetric about its peak, remains lacking. Additionally, for reliable projections, it is necessary to accommodate exogenous variables driving groundwater pumping in a unified framework, especially crop production and groundwater recharge, because, if their interaction causes delays and hysteretic phase–space loops, then relations between these two variables will be missed (16).

To mathematically explain the emergence of peak grain production, or peak grain, and its links to peak water, a dynamical system was formulated where groundwater availability and crop production are dynamic variables and are subject to groundwater recharge. This approach was applied to groundwater use and crop production on the HPA of Texas, Kansas, and Nebraska. Lags between peak water and peak grain and the asymmetric trends of groundwater withdrawal and crop production about their peaks were projected and related to aquifer lifespan. The approach additionally offers a perspective on what technological disruptions, such as the introduction of low-energy precision application (LEPA) irrigation in Texas, mean in the context of peak water and peak grain. The model projections also offer an outlook on water availability and crop production on the HPA through 2050. While the model formulation is sufficiently general and transferable to other regions, frequent records of groundwater pumping and irrigated crop area and production make the HPA both ideal and pragmatic for exploring such a "coarse-grained" or large-scale approach.

Theory and Application to the HPA

The proposed dynamical system strikes a balance between the mathematical tractability of the feedbacks present in many groundwater-dependent irrigation systems and the number of parameters or coefficients needed to describe the groundwater–grain production system. The model has three state variables: planted groundwater-irrigated area (A, hectares), accessible groundwater volume for irrigation (W, cubic kilometers), and annual rate of grain production by weight (C, tons per year). The accessible volume is the volume deemed economically viable for wells to tap into where they exist. The model describes the state of the groundwater–grain production compartments and their interaction as

$$\frac{\mathrm{d}W}{\mathrm{d}t} = -k_1\, C\, W + R\, A_{\mathrm{HPA}} + k_4\, \frac{\mathrm{d}A}{\mathrm{d}t}, \qquad [1]$$

$$\frac{\mathrm{d}C}{\mathrm{d}t} = k_2\, C\, W - k_3\, C = k_2 \left(W - \frac{k_3}{k_2} \right) C, \qquad [2]$$

where A, W, and C are functions of time t, and the four parameters k_1, k_2, k_3, and k_4 are positive constants (Table 1). In Eq. **1**, the first term is the rate of groundwater withdrawal, the second term is the aquifer recharge rate (where aquifer recharge is the product of a time-averaged, area-normalized rate R with the area of the HPA underlying the region of interest A_{HPA}), and the third term is the increase in accessible groundwater when the irrigation area increases and new wells are installed. In Eq. **2**, the first term encodes the increase in annual crop production balanced by the second term that sets a limit on C growth.

The first terms in Eqs. **1** and **2** drive expected and necessary endogenous feedbacks on W and C. Higher water withdrawal rates ($k_1\, C\, W$; cubic kilometers per year) and a faster crop production (C) are caused by a large preexisting W when wells are first drilled and maintained by an elevated C long after irrigated agriculture started expanding, an elevated C that generates economic returns. The economic returns due to high C are reinvested into acquiring efficient water applicators and implementing techniques that increase the economic value of each unit volume of water, including applying fertilizers and pesticides, thereby incentivizing further pumping. In contrast, deeper water levels (lower W) increase pumping costs. These costs dampen groundwater withdrawal rates and reduce the value of marginal increases in crop production. This symmetry between the effects of high W, low C and high C, low W on groundwater pumping and annual crop production explains why the realistic feedbacks emerge from multiplying those terms.

On their own, the first terms on the right-hand side of Eqs. **1** and **2** produce a linear relation between W and C trends (i.e., $dW/dC = -k_1/k_2$). The remaining three processes generate the boom–bust cycles and delays between W and C.

The first exogenous process is the groundwater recharge rate $R\, A_{\mathrm{HPA}}$, a process with significant spatial gradients and one that is subject to temporal variations where surface water–groundwater interactions are significant. Recharge ranges from 7.9 mm/y in the southern HPA to 18 mm/y in the central HPA and up to 64 mm/y in the northern HPA (17). These estimates of R include both direct infiltration following precipitation and focused recharge from streams and ephemeral lakes. While the approach includes latitudinal gradients, it does not consider longitudinal gradients in R, a simplification that is most

Table 1. Parameter values for the models shown in Fig. 1

	Nebraska	Kansas	Texas, pre-LEPA	Texas, post-LEPA	Units
k_1	8.6e-9	6.2e-9	7.2e-9	5.5e-9	tons^{-1}
k_2	5.6e-4	3.3e-4	2.9e-4	3.2e-4	$\mathrm{km}^{-3}\ \mathrm{y}^{-1}$
k_3	—	0.020	0.075	0.046	y^{-1}
k_4	0.96	7.4	—	—	cm
W_0	90	33	430	310	km^3
C_0	2.3e6	4.2e6	3.0e6	3.3e6	tons y^{-1}

The initial values W_0 and C_0 are taken at year 1955 for Texas (pre-LEPA) and Nebraska, 1972 for Kansas, and 1986 for Texas (post-LEPA). Hyphens denote unused parameters for the given state (see *Materials and Methods*). The e'a' notation denotes the order of magnitude, that is, 10^a.

significant for Nebraska where R increases quasi-monotonically eastward (18), and it does not consider temporal variations in R or feedbacks from groundwater pumping onto R. In Nebraska, where groundwater and surface water resources are connected, groundwater-based irrigation is initially derived from groundwater storage but, later, more from stream capture that ameliorates groundwater level declines over time (19, 20). This work also neglects regulatory aspects of water management such as the Republican River compact between Colorado, Kansas, and Nebraska (21) that results in Nebraska pumping groundwater for river discharge to meet the compact requirements.

The second exogenous process is groundwater-irrigated area expansion $k_4 \mathrm{d}A/\mathrm{d}t$ (where the equation governing A is provided in *Materials and Methods*). Increases in A signify new wells being drilled. This association relies on long-range water transport not being economically viable, an association that means that all pumped groundwater is used locally for C production. The area was kept constant in Texas because irrigated agriculture area expansion ceased in the mid-1960s. In Kansas, the irrigated area continued expanding until the early 1990s. The irrigated area is still increasing in Nebraska, and the area equation projects it to plateau at about 25% of the 16.2 million hectares of the state overlying the HPA by 2050 (*SI Appendix*, Fig. S1) and correctly leaves out Nebraska's large nonirrigable lands such as the Sand Hills (18).

The additional endogenous process is the $k_3\ C$ term that sets a condition on whether W promotes increases or decreases in the rate of crop production and specifies peak grain at $W = k_3/k_2$. The rate of change of C, however, is set by the value of C itself (Eq. **2**). This process ensures that, as water levels decline, irrigated area reaches full capacity, and crop yields stagnate, the marginal value of additional pumping to increase dC/dt is reduced.

The mathematical structure of the proposed model resembles a Lotka–Volterra or predator–prey interaction (22, 23) where annual crop production acts as a predator on groundwater resources that have two external sources: R and $k_4 \mathrm{d}A/\mathrm{d}t$. The model also resembles coupled chemical reactions metaphorically labeled as "autocatalytic" because the loss term in the "water reaction" acts as a gain in the "crop reaction." Despite the number of processes modeled in this approach, fitting this model requires, at most, one additional coefficient compared to having two independent Hubbert curves for crop production and water level time series (Table 1; equation in legend of Fig. 1). Moreover, the model focuses on groundwater withdrawals rather than groundwater depletion. This allows the model to describe conditions where groundwater depletion is negligible, such as in the northern HPA where much of the pumped groundwater comes from stream capture (24). Finally, by keeping k_1, k_2, k_3, and k_4 constant, processes meriting independent consideration were omitted for parsimony but without loss of generality.

Findings

Kansas saw a rapid increase in irrigated crop area starting from the early 1970s reaching a steady state in the 1980s at 1.2 million hectares (*SI Appendix*, Fig. S2). This increase drove a rise in groundwater withdrawal that then ceased when peak water occurred in the 1990s, followed by a rapid decline (Fig. 1*A* and *SI Appendix*, Fig. S3). Despite this decline, irrigated crop production still increased, albeit at a reduced rate in recent years. During this time, due to a yield advantage of 4 tons/ha over its nonirrigated counterpart (12.3 tons/ha versus 8.2 tons/ha) (25, 26), irrigated corn area doubled (283,000 ha to 567,000 ha) while winter wheat decreased to a third (364,000 ha to 121,000 ha) and sorghum decreased dramatically (324,000 ha to 40,000 ha) (27). Because irrigated corn has higher yield than irrigated wheat (7.4 tons/ha) and irrigated sorghum (9.9 tons/ha), the total rate of irrigated crop production by weight continued to rise (Fig. 1*A*) (26). Grain production trends are projected to decline starting in 2018, thus lagging the decline in groundwater withdrawal by 24 y.

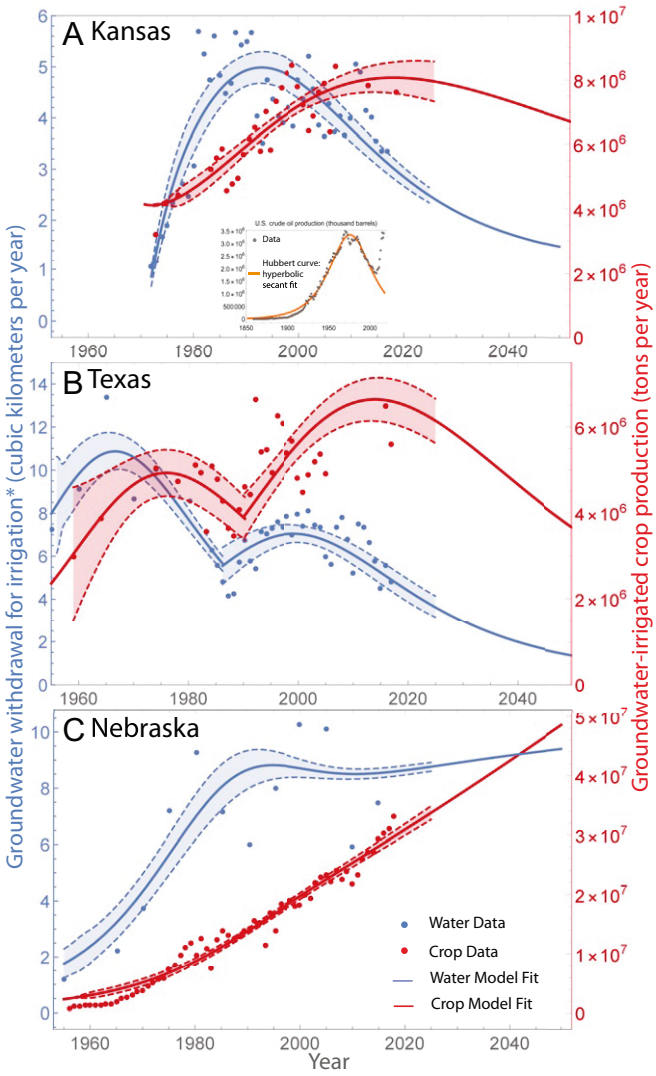

Fig. 1. Model fitting and forecasts for (*A*) Kansas, (*B*) Texas, and (*C*) Nebraska. For each state, there is a fit for groundwater withdrawal for irrigation (blue) and another for groundwater-irrigated crop production (red). *Inset* shows the Hubbert curve (orange) for US crude oil production data (gray). The mathematical form of a symmetric Hubbert curve is $y(t) = y_{max}\left[e^{-\omega(t-\tau)} + e^{\omega(t-\tau)}\right]^{-1}$, where y_{max}, ω, and τ are three parameters determined from data fitting. In *B*, Texas saw a shift in trends in the second half of the 1980s due to technological and energy price disruptions (see *Findings*). The preshift trends and postshift trends are fitted independently, and the change in model parameter values is shown in Table 1. The shaded regions around the fits represent 90% confidence bands as a result of parameter fitting uncertainty. All fits have an adjusted r-square value of 0.98. See *Materials and Methods* and *SI Appendix* for data processing information and sources. *: For Nebraska and pre-1975 Texas, groundwater use for irrigation data were used.

In Texas, increasing pumping costs (28) and ever-decreasing groundwater levels (6, 18) led to a steep decline in groundwater extraction starting in 1966. Peak crop production followed in 1975—a 9-y gap. However, the widespread adoption of sprinklers starting in the mid-1960s, especially LEPA (*SI Appendix*, Fig. S4), caused a rebound in the rate of water extraction and crop production, because energy costs decreased and profit

margins increased (Fig. 1*B* and *SI Appendix*, Fig. S3). This rebound gradually "gained steam" starting in the early 1980s.

Even though advanced sprinkler adoption was concurrent in the three states, it caused a "disruption" to the dynamical systems model only in Texas. A technological innovation that significantly alters an existing trend is dubbed a disruption (29). Sprinkler adoption in Texas in the early 1980s reversed the groundwater withdrawal and crop production collapse into an expansion. To account for such a disruption with the current approach, the model is refit with the postdisruption trends. While revising the four model parameters to be time dependent is possible, a "hard threshold" or an abrupt change in parameter values may be justified in some circumstances (see *Materials and Methods*).

The model parameters were refitted with the new trends pre- and post-1985, the year in which the sprinkler adoption rate was half its value today (*SI Appendix*, Fig. S4). Only k_3 saw a reduction with 90% confidence (–44%), while k_1 and k_2 did not change significantly (Table 1). This is a result of the structure of Eq. **2** wherein the W at which the annual crop production peaks is determined by parameter k_3. A smaller k_3 indicates that a given available amount of water (W) can support greater crop production owing to increased irrigation efficiency (Eq. **2**). The new fit explained the occurrence of a second peak water that occurred in 1997 and a second peak grain in 2012—a 15-y lag (Fig. 2).

The effect of a future innovation on groundwater withdrawals and crop production depends on the adoption time and its impact on crop yield, water use efficiency, and economic returns. Even though the timing and impact of future enhancements and innovations are difficult to predict, a sensitivity analysis of Texas groundwater pumping and crop production in 2050 to reductions in k_3 is possible (*SI Appendix*, Fig. S5). A 50% reduction in k_3 by 2025 would instigate a third peak grain, but it still would not be sufficient for crop production in 2050 to match its second peak. Generally, the model results in linear decreases in crop production in 2050 with later innovation adoption times (*SI Appendix*, Fig. S5). Strikingly, groundwater withdrawal magnitudes in 2050 are almost insensitive to k_3 reductions. This insensitivity is due to low recharge and high depletion even as early as 2015; some regions of Texas have seen their water levels decline by as much as 50 m (6).

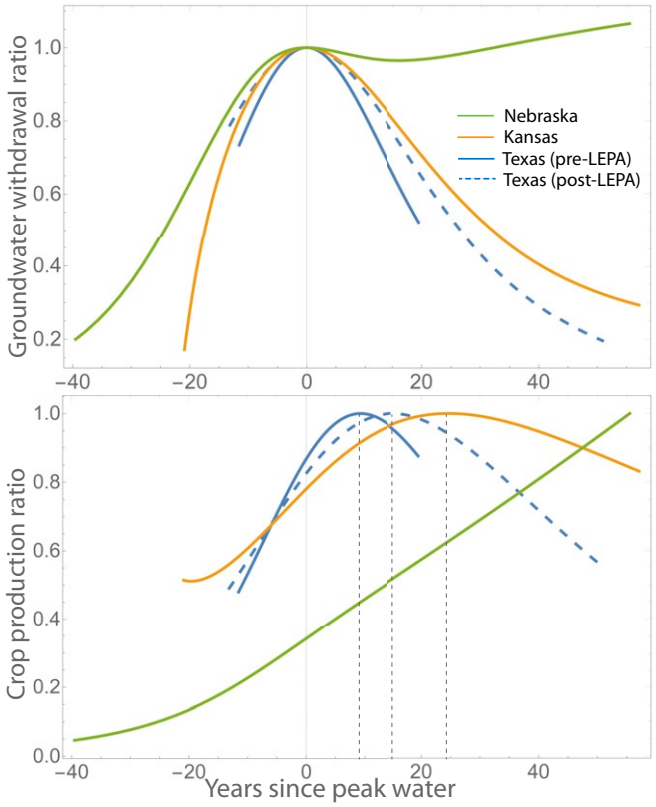

Fig. 2. Lags between peak water and peak grain and asymmetries about the peaks. (*Top*) Trends in groundwater extraction for the three states normalized by their respective peak values. (*Bottom*) Normalized crop production rates by peak crop production values. For Nebraska, peak crop production is the last production data point (2018). The abscissa is shifted in time such that peak water occurs at $t = 0$ for all three states.

Nebraska, the most northern of the three states, has the largest surface area overlying the HPA, the highest recharge rate, and the largest volume of saturated aquifer material underneath it (6, 15). Although its harvested irrigated area steadily increased ($dA/dt > 0$; *SI Appendix*, Fig. S2), the rate of groundwater irrigation use reached a quasi-steady state around year 2000 at about 10 $km^3\ y^{-1}$ (Fig. 1*C*). This decreasing water extraction rate per unit area is likely driven by widespread LEPA adoption around the end of the 1980s (28, 30, 31). No peak grain occurrence is projected before 2050, as A and C are expected to continue increasing beyond 2050. A projected 8% increase in R for Nebraska due to climate change (17) further supports this prediction.

The increasing asymmetry in groundwater use about peak water and the lag between peak water and peak grain are most apparent in Fig. 2. There is a positive latitudinal gradient in asymmetries and lags. Pre-LEPA Texas, post-LEPA Texas, and Kansas observed 9-y, 15-y, and 24-y lags, respectively. Furthermore, compared to the other states, the two Texas "booms" followed by "busts" resemble the Hubbert curve the most (compare Fig. 1 *B* and *Inset*). This analysis suggests that lower recharge rates and more-aggressive pumping (with respect to available resources) manifest themselves as smaller lags between peak water and peak grain and more-symmetric withdrawal and production trends.

Peak groundwater use for pre-LEPA Texas was at such a high and unsustainable value (13 $km^3\ y^{-1}$ in 1965; Fig. 1*B*) that it was halved by 2018 and is projected to decrease to about 90% of peak value by 2050. The peak Texas groundwater withdrawal rate is 30% higher than the sustained withdrawal rate of Nebraska, even though it possesses about half of Nebraska's surface area overlying the HPA, a sixth of its saturated aquifer volume, a lower recharge rate, and lower specific yield of the underlying aquifer material (6, 17, 32). This underscores how groundwater use history contributes to a severe collapse in groundwater extraction, twice in Texas (*SI Appendix*, Table S1). These projections would deviate from future trends if another unpredictable disruption occurs in the HPA (29).

The proposed approach was used to assess increases in aquifer lifespan due to groundwater withdrawal reduction programs such as the Local Enhanced Management Area program in Kansas (*SI Appendix*, *Supplementary Text*) (33). The dynamical systems approach can also be extended to explore groundwater withdrawal–crop production systems worldwide. For example, groundwater in the alluvial aquifer systems of northwestern India is an indispensable source of both drinking and agricultural water for some of India's most agriculturally productive land. Intense extraction of this resource has posed challenges on water quantity but also quality; high salinity and concentrations of fluoride, nitrate, and uranium are widespread in this aquifer (34, 35). Because the recycling of groundwater through irrigation increases the concentrations of these contaminants, a new feedback term in Eq. **1** can be introduced to capture such effects on crop production. Other withdrawal–agriculture systems are driven not by local or global food demand but by government stimulation programs, as in Saudi Arabia (36). Such a system

requires these government incentives to be parameterized as new source terms for either W, C, or both.

Conclusions

Irrigated agricultural production in the US High Plains has pursued growth beyond sustainable limits set by groundwater resources and their recharge (2). Delays in introducing adequate responses to approaching these limits, through enforcement of policies (37) and extensive water use reporting (21), have resulted in unsustainable rates of groundwater use causing the phenomenon of peak water followed by peak grain. The proposed approach has shown that the consequence of these peaks is an eventual collapse in withdrawal and production trends. It has also revealed that the lag between the peaks and the asymmetry of the trends increase as the historical magnitude of groundwater withdrawals is more commensurate with recharge and available resources. On the HPA, coarser soils in the Sand Hills (increasing recharge) (18) and surface water capture (19) have endowed Nebraska with a long aquifer lifespan, whereas, in Texas, aggressive use of this resource has twice resulted in rapid crashes following peak water and peak grain within only four decades.

In the future, technological innovations (28) and adoption of high-yield, low water use crops with reduced irrigation requirements (26) would actively alleviate aquifer depletion. Current groundwater withdrawal trends and future climate conditions affecting groundwater recharge rates (7, 17) and crop yields (38) may force southern High Plains croplands to revert to dryland agriculture and allow the northern High Plains to balance out the deficits in overall crop production. However, groundwater quality concerns might arise, as intense production and fertilizer use are increasing nitrate concentrations, especially in regions of high recharge (39). Environmental concerns surrounding surface freshwater resources, such as the extirpation of fish assemblages (24), may further hamper groundwater-sourced irrigation in the northern High Plains through adjudication.

Finally, the proposed dynamical system was successful in considering multiple processes and disentangling their effects on long-term groundwater withdrawal and crop production on the HPA. The general patterns of withdrawal and production that are elucidated here apply to any aquifer, whether pumping for crop production outweighs or balances groundwater recharge. It is also possible to represent additional drivers such as groundwater quality and economic incentives. Thus, the framework adopted herein is transferable to groundwater-irrigated agriculture systems worldwide toward promoting sustainable groundwater management.

Materials and Methods

Data sourcing and processing are detailed in this section and are complemented by a flowchart (*SI Appendix*, Fig. S6).

Groundwater Data. Data on annual Kansas groundwater withdrawal for irrigation were compiled from an online database curated by the Kansas Geological Survey (40). For Texas, annual post-1974 groundwater withdrawal estimates are available through the Texas Water Development Board (TWDB). Pre-1974 Texas and Nebraska lack long-term groundwater withdrawal reporting or estimation. In this case, the US Geological Survey (USGS) Water Data for the Nation (WDN) was used, in which estimates were updated every 5 y (30). The USGS water data are for the entire states. For Texas, to estimate water use for the region of interest (see specific counties below), the whole state's groundwater use was multiplied by 80%. This factor was obtained using the mean of the ratios of Texas HPA groundwater withdrawals to the whole state's withdrawals after 1975 (30, 41). Volumes were all converted to cubic kilometers. While losses occur when water is conveyed from pumping source to destination, this contribution is small and does not affect the conclusions.

Crop Data. Nebraska, Kansas, and Texas irrigated crop production and planted or harvested irrigated area data were obtained from census and survey reports from the National Agricultural Statistics Service of the US Department of Agriculture (25). When both a survey estimate and a census value exist for the same data item in the same year, the census value is used. Planted irrigated area data for the crops of interest were used to capture the drilling of new wells in previously untapped regions of the HPA. Because Nebraskan yearly planted irrigated area data were insufficient before the mid-1980s, harvested irrigated area data were used. Even though harvested area is smaller than planted area, this discrepancy has no effect on the conclusions, as planted and harvested areas increase at roughly the same rate (dA/dt in Eq. **1**). The recharge area in Eq. **1** (A_{HPA}) is the total area of the HPA underlying each state (32).

For all three regions, corn for grain, sorghum, and winter wheat data were used for crop production. Additionally, grain soybean was used for Kansas and Nebraska, and cotton was used for Texas. Weights were converted from bushels and bales to metric tons. Counties included in the Texas High Plains are the components of the TWDB Groundwater Management Areas 1 and 2 (42). Kansas High Plains counties are Cheyenne, Clark, Comanche, Decatur, Edwards, Finney, Ford, Gove, Graham, Grant, Gray, Greeley, Hamilton, Harvey, Haskell, Hodgeman, Kearny, Kingman, Kiowa, Lane, Logan, McPherson, Meade, Morton, Norton, Pawnee, Pratt, Rawlins, Reno, Scott, Sedgwick, Seward, Sheridan, Sherman, Stafford, Stanton, Stevens, Thomas, Wallace, and Wichita counties.

Model Calibration. The "ParametricNDSolveValue" function of Mathematica (43) was used to define the parametric differential equation presented in *Theory and Application to the HPA*. Numerical integration was performed with the implicit backward differentiation formulas. Using the "NonlinearModelFit" function, least-squares curve fitting was performed with the "Levenberg–Marquardt" method. The target was to achieve the highest possible adjusted coefficient of determination (r squared) that takes into account the number of parameters. Mean prediction band values at a 90% confidence level were obtained for the fits. The mean prediction band values accounted for errors in parameter estimates. These band values were then interpolated with a cubic spline to obtain the bands shown in Fig. 1.

The area equation (see below) was first fitted with irrigated area planted or harvested data, and a continuous function of A in time was obtained, but only for Kansas and Nebraska, because irrigated crop area expansion ceased around the beginning of the study time frame for Texas. Second, irrigation groundwater pumpage or use data ($k_1\,C\,W$) and annual crop production data (C) were used to simultaneously fit Eqs. **1** and **2**. In cases such as in Nebraska, where more data points exist for irrigated crop production (yearly) compared to groundwater use (5-y intervals), the less frequent data were weighted appropriately to balance out the simultaneous fitting. For Texas, separate fits were performed between 1955 and 1988 and between 1988 and 2017. This is to capture energy price and technological disruptions driven by the adoption of LEPA as detailed in *Findings* (see below; *SI Appendix*, Fig. S4).

The Area Equation. The expansion of groundwater irrigation is captured by the area equation $dA/dt = r_0\,(1 - A/A_f)$. This process is terminated when the final value for irrigated area A_f is reached over a time scale set by $1/r_0$. It is fit independently from Eqs. **1** and **2**, and it constrains future values of A to physically reasonable magnitudes and separates out externally driven reductions in A (such as the late 1980s in Texas; *SI Appendix*, Fig. S1). Because neither C nor W has a strong feedback on A here, it is treated as an externally supplied time-dependent "forcing" in the $dW(t)/dt$ budget. Its dynamics are determined from independent data sources that do not use either the $C(t)$ or $W(t)$ time series.

Surface Water–Groundwater Partitioning. Surface water irrigation constituted less than 2% of irrigated agricultural water in the Texas High Plains from 1974 to 2017 (*SI Appendix*, Fig. S7*C*) (44) and less than 4% in the Kansas High Plains from 1985 to 2015 (*SI Appendix*, Fig. S7*B*) (30). For these regions, irrigated grain production is assumed to be fully groundwater irrigated. For Nebraska, surface water contributed a monotonically decreasing proportion, from a maximum of 67% of irrigation water in 1955 to a minimum of 11% of irrigation water in 2015 (*SI Appendix*, Fig. S7*A*). To exclude surface water-irrigated crop production, data on the fraction of the irrigation water from surface resources in Nebraska were used. Such data are provided at a 5-y resolution through the USGS WDN dataset (30). These 5-y data were then linearly interpolated to achieve a yearly estimate of surface water fraction of the total. Then, irrigated crop production was multiplied by the fraction of water from groundwater sources. The underlying

argument for this method is that irrigated crop yields are invariant relative to the source of water used.

Parameter k_3 for Nebraska. Parameter k_3 for Nebraska was set to zero in the model runs, because it was deemed a redundant parameter in Nebraska's model fitting. The 90% CI for k_3 in Nebraska's case was $[-0.004, 0.008]$. Since the fitting was indifferent to the sign of k_3, the term $k_3 C$ was omitted from Nebraska's set of equations. This means that future data points are necessary to identify k_3 for Nebraska because 1) water levels have not changed significantly since the mid-19th century and 2) the crop production trends have increased in a quasi-linear fashion up to today since 1970.

The Role of Model Parameters in Generating Asymmetry about the Peaks. In the limit of $k_3 = 0$ and negligible recharge ($R = 0$), and at an equilibrium $A = A_f$ (meaning that water is now strictly a nonrenewable resource), the dynamical systems model reduces to $C(t) = -(k_2/k_1)W(t) + I_c$, where I_c is an integration constant that varies from state to state. Hence, onset of hysteretic patterns in the $C - W$ phase space (*SI Appendix*, Fig. S8) and lags between peak C and peak W can be attributed to the magnitudes of k_3 and R when $A = A_f$. Because R is kept constant, only k_3 explains the longer lags observed from pre-LEPA to post-LEPA Texas.

Diffusion of New Technologies. Diffusion of new technologies in populations is routinely approximated by a logistic function (i.e., $y(t) = y_{max}[1 + (y_{max}/y_{50} - 1)e^{-r(t-\tau)}]$) characterized by the time scale $1/r$ (45). When this time scale is short relative to the study duration, as is the case for sprinklers in Texas (8.3 y; *SI Appendix*, Fig. S4), the logistic function can be approximated by a jump (no adoption to full adoption) centered at 50% of maximum adoption rate.

Data Availability. All study data are included in the article and *SI Appendix*.

ACKNOWLEDGMENTS. This paper stems from discussions during the Ettersburg Ecohydrology Workshop in Germany (October 2018), with the corresponding manuscript preparation ensuing in subsequent months. The workshop was funded by the UNIDEL Foundation, Inc. and the University of Delaware. Accordingly, partial support for this paper derived from funding for the workshop. A.M. was supported by the US NSF (Grants NSF-AGS-1644382 and NSF-IOS-175489).

1. W. Ripl, Water: The bloodstream of the biosphere. *Philos. Trans. R. Soc. Lond. Ser. B Biol. Sci.* **358**, 1921–1934 (2003).
2. Y. Wada *et al.*, Global depletion of groundwater resources. *Geophys. Res. Lett.* **37** L20402 (2010).
3. P. D'Odorico *et al.*, The global food-energy-water nexus. *Rev. Geophys.* **56**, 456–531 (2018).
4. F. Harris *et al.*, The water footprint of diets: A global systematic review and meta-analysis. *Adv. Nutr.* **11**, 375–386 (2020).
5. F. García Suárez, L. Fulginiti, R. Perrin, What is the use value of irrigation water from the High Plains Aquifer? *Am. J. Agric. Econ.* **101**, 455–466 (2019).
6. V. L. McGuire, "Water-level and recoverable water in storage changes, high plains aquifer, predevelopment to 2015 and 2013–15" (Scientific Investigations Rep. 2017–5040, US Geological Survey, 2017).
7. B. R. Scanlon, R. C. Reedy, J. B. Gates, P. H. Gowda, Impact of agroecosystems on groundwater resources in the Central High Plains, USA. *Agric. Ecosyst. Environ.* **139**, 700–713 (2010).
8. M. A. Maupin, N. L. Barber, "Estimated withdrawals from principal aquifers in the United States, 2000, U.S" (Geol. Surv. Circular. 1279, US Geological Survey, 2005).
9. M. Hubbert, "Energy resources: A report to the committee on natural resources" (Rep. PB-222401, National Research Council, Washington, DC, 1962).
10. US Energy Information Administration, "U.S. field production of crude oil" (US Energy Information Administration, 2020). https://www.eia.gov/dnav/pet/hist/LeafHandler.ashx?n=PET&s=MCRFPUS2&f=M. Accessed 31 January 2020.
11. A. Bartlett, An analysis of us and world oil production patterns using Hubbert-style curves. *Math. Geol.* **32**, 1–17 (2000).
12. S. Sorrell, J. Speirs, Hubbert's legacy: A review of curve-fitting methods to estimate ultimately recoverable resources. *Nat. Resour. Res.* **19**, 209–230 (2010).
13. P. H. Gleick, M. Palaniappan, Peak water limits to freshwater withdrawal and use. *Proc. Natl. Acad. Sci. U.S.A.* **107**, 11155–11162 (2010).
14. D. Steward *et al.*, Tapping unsustainable groundwater stores for agricultural production in the High Plains Aquifer of Kansas, projections to 2110. *Proc. Natl. Acad. Sci. U.S.A.* **110**, E3477–E3486 (2013).
15. D. Steward, A. Allen, Peak groundwater depletion in the High Plains Aquifer, projections from 1930 to 2110. *Agric. Water Manag.* **170**, 36–48 (2016).
16. P. Turchin, A. Korotayev, Population dynamics and internal warfare: A reconsideration. *Soc. Evol. Hist.* **5**, 112–147 (2006).
17. T. Meixner *et al.*, Implications of projected climate change for groundwater recharge in the western United States. *J. Hydrol.* **534**, 124–138 (2016).
18. B. R. Scanlon *et al.*, Groundwater depletion and sustainability of irrigation in the US High Plains and Central Valley. *Proc. Natl. Acad. Sci. U.S.A.* **109**, 9320–9325 (2012).
19. L. Konikow, S. Leake, Depletion and capture: Revisiting "the source of water derived from wells."*Groundwater* **52**, 100–111 (2014).
20. I. de Graaf, T. Gleeson, L. van Beek, E. Sutanudjaja, M. Bierkens, Environmental flow limits to global groundwater pumping. *Nature* **574**, 90–94 (2019).
21. M. Sophocleous, Review: Groundwater management practices, challenges, and innovations in the High Plains aquifer, USA—Lessons and recommended actions. *Hydrogeol. J.* **18**, 559–575 (2010).
22. A. Lotka, Elements of physical biology. *Sci. Prog. Twent. Century (1919–1933)* **21**, 341–343 (1926).
23. V. Volterra, Variazioni e fluttuazioni del numero d'individui in specie animali conviventi. *Mem. R. Acaad. Naz. dei Lincei.* **2**, 31–113 (1926).
24. J. S. Perkin *et al.*, Groundwater declines are linked to changes in Great Plains stream fish assemblages. *Proc. Natl. Acad. Sci. U.S.A.* **114**, 7373–7378 (2017).
25. National Agricultural Statistics Service, USDA/NASS quickstats ad-hoc query tool. https://www.mssoy.org/uploads/files/soy-yld-national-2013-2018-nass.pdf. Accessed 28 October 2019.
26. M. Kukal, S. Irmak, Irrigation-limited yield gaps: Trends and variability in the United States post-1950. *Environ. Res. Commun.* **1**, 061005 (2019).
27. US Department of Agriculture, "2018 state agriculture overview for Kansas" (US Department of Agriculture, 2018). https://www.nass.usda.gov/Quick_Stats/Ag_Overview/stateOverview.php?state=KANSAS. Accessed 12 December 2019.
28. S. Smidt *et al.*, Complex water management in modern agriculture: Trends in the water-energy-food nexus over the High Plains Aquifer. *Sci. Total Environ.* **566**, 988–1001 (2016).
29. P. H. Gleick, Transitions to freshwater sustainability. *Proc. Natl. Acad. Sci. U.S.A.* **115**, 8863–8871 (2018).
30. US Geological Survey, "USGS water use data for the nation" (US Geological Survey, 2020). https://waterdata.usgs.gov/nwis/wu. Accessed 4 February 2020.
31. P. Colaizzi, P. Gowda, T. Marek, D. Porter, Irrigation in the Texas high plains: A brief history and potential reductions in demand. *Irrig. Drain.* **58**, 257–274 (2009).
32. V. McGuire, K. Lund, B. Densmore, "Saturated thickness and water in storage in the High Plains aquifer, 2009, and water-level changes and changes in water in storage in the High Plains aquifer, 1980 to 1995, 1995 to 2000, 2000 to 2005, and 2005 to 2009" (Rep. 2012-5177, US Geological Survey, 2012).
33. J. Deines, A. Kendall, J. Butler, D. Hyndman, Quantifying irrigation adaptation strategies in response to stakeholder-driven groundwater management in the US High Plains aquifer. *Environ. Res. Lett.* **14**, 0044014 (2019).
34. A. MacDonald *et al.*, Groundwater quality and depletion in the Indo-Gangetic basin mapped from in situ observations. *Nat. Geosci.* **9**, 762–766 (2016).
35. R. Coyte, A. Singh, K. Furst, W. Mitch, A. Vengosh, Co-occurrence of geogenic and anthropogenic contaminants in groundwater from Rajasthan, India. *Sci. Total Environ.* **688**, 1216–1227 (2019).
36. A. Youssef *et al.*, Natural and human-induced sinkhole hazards in Saudi Arabia: Distribution, investigation, causes and impacts. *Hydrogeol. J.* **24**, 625–644 (2016).
37. R. Kaiser, F. Skiller, Deep trouble: Options for managing the hidden threat of aquifer depletion in Texas. *Tex. Tech Law Rev.* **32**, 249–304 (2001).
38. H. Pei *et al.*, Impacts of varying agricultural intensification on crop yield and groundwater resources: Comparison of the North China Plain and US High Plains. *Environ. Res. Lett.* **10**, 044013 (2015).
39. A. Lane *et al.*, Long-term (1970s–2016) changes in groundwater geochemistry in the High Plains aquifer in south-central Kansas, USA. *Hydrogeol. J.* **28**, 491–501 (2019).
40. Kansas Geological Survey, "WIMAS query page" (2019). https://hercules.kgs.ku.edu/geohydro/wimas/index.cfm. Accessed 20 November 2019.
41. C. G. Turner, K. McAfee, S. Pandey, A. Sunley "Irrigation metering and water use estimates: A comparative analysis, 1999-2007" (No. 378, Texas Water Development Board, 2011).
42. Texas Water Development Board, "Groundwater management areas" (2019). https://www.twdb.texas.gov/groundwater/management_areas/index.asp. Accessed 5 December 2019.
43. Wolfram Research, Inc., Mathematica, (Version 12.1, Wolfram Research, Inc., Champaign, IL, 2020).
44. Texas Water Development Board, "Historical water use estimates" (2020). https://www.twdb.texas.gov/waterplanning/waterusesurvey/estimates/index.asp. Accessed 2 February 2020.
45. E. Rogers, *Diffusion of Innovations* (Simon & Schuster, 2010).